Journal of Materials Chemistry C

Accepted Manuscript

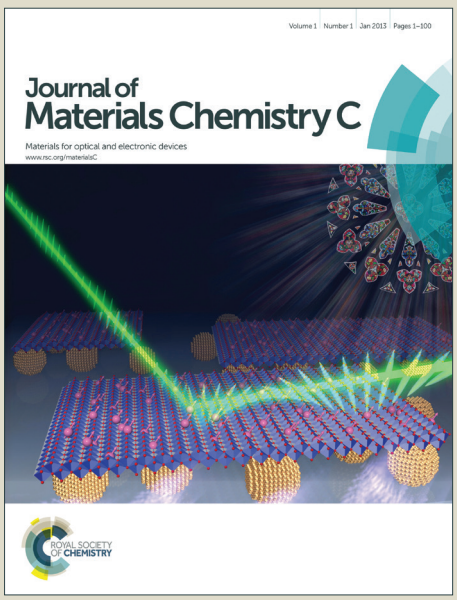

ROYAL SOCIETY OF CHEMISTRY

www.rsc.org/materialsC

Journal Name

RSCPublishing

ARTICLE

Solution-Processable Host Material of 1,3-Bis{3-[3-(9-carbazolyl)phenyl]-9-carbazolyl}benzene and its Application in Organic Light-Emitting Diodes Employing Thermally Activated Delayed Fluorescence

Cite this: DOI: 10.1039/x0xx00000x

Received ooth January 2012,
Accepted ooth January 2012

DOI: 10.1039/x0xx00000x

www.rsc.org/

Yoshitake Suzuki,[a,b] Qisheng Zhang[a] and Chihaya Adachi[a,]*

Solution-processed organic light-emitting diodes (OLEDs) that employed an efficient green thermally activated delayed fluorescence dopant of (4s,6s)-2,4,5,6-tetra(9H-carbazol-9-yl)isophthalonitrile (4CzIPN) and small molecular hosts were thoroughly investigated. We demonstrated that increasing the electron injection and transport capabilities of the electron transport layers as well as the glass transition temperature (T_g) of the host material can significantly improve the half-life of the OLEDs. Using a novel host material of 1,3-bis{3-[3-(9-carbazolyl)phenyl]-9-carbazolyl}benzene (CPCB) with a high triplet energy level of 2.79 eV and a high T_g of 165 °C, a solution-processed 4CzIPN-based OLED achieved an external electroluminescence quantum efficiency of 10% and a half-life of nearly 200 hours with an initial luminescence of 1000 cd/m^2. This was comparable to a device that used a dry-processed emissive layer.

1. Introduction

Metal free materials that display thermally activated delayed fluorescence (TADF) have received significant attention in recent years because of their epoch-making molecular design that incorporates simple aromatic compounds. Owing to the small energy gap between the lowest singlet (S_1) and triplet (T_1) excited states, TADF emitters in organic light-emitting diodes (OLEDs) can upconvert triplet excitons that have a long lifetime into an emissive singlet state, realizing high external electroluminescence (EL) quantum efficiencies (EQEs). We demonstrated that all green, orange-red and blue TADF emitters can achieve nearly 100% photoluminescence quantum yield (PLQY) and the devices realized high EQEs that were comparable to the conventional phosphorescent OLEDs (PHOLEDs) employing Ir-based phosphors.[1f,1g,1i,2] Since the cost of TADF materials can be much lower than that of the phosphorescent materials, TADF-based OLEDs are expected to be the third generation OLEDs after PHOLEDs.

Besides material cost, device fabrication procedures are also a serious issue. In particular, solution coating processes have been widely developed instead of vacuum deposition (dry) processes because they are simple and are low cost, leading to the removal of high vacuum processing, cheaper equipment costs, and capability for large area scalability.[3-5] However, the industrialization of solution-processed OLEDs has been largely delayed because of their inferior EQEs, device reproducibility, and device reliability. In the last decade, significant efforts have been devoted to explore solution-processed PHOLEDs.[4,5] In particular, solution-processed PHOLEDs using small molecular hosts have achieved high EQEs that are comparable to dry-processed PHOLEDs.[5] In comparison with polymeric hosts, small molecular hosts have been used to achieve higher triplet energy levels and better dispersion of the guest emitters.[5d,5f-h] However, the operational stability of solution-processed PHOLEDs with small molecular hosts has been hardly reported by academic institutions.[5c,5e]

In this study, we prepared TADF-based OLEDs using spin-coating. Green-emitting (4s,6s)-2,4,5,6-tetra(9H-carbazol-9-yl)isophthalonitrile (4CzIPN) was used as an emitter because of its high performance in dry-processed OLEDs and good solubility in dichloromethane (>30 mg/mL).[1f] Herein, we systematically studied the operational stability of solution-processed TADF-based OLEDs using small molecular hosts. To improve reliability, we applied a new host material of 1,3-bis{3-[3-(9-carbazolyl)phenyl]-9-carbazolyl}benzene (CPCB) that has a high T_1 and glass-transition temperature (T_g), and achieved stable and efficient solution-processed TADF-based OLEDs.

2. Experimental

2.1 General information

All solvents and starting materials were purchased from commercial sources and were used as received. OLED materials 2,4,6-tris(biphenyl-3-yl)-1,3,5-triazine (T2T) and 2,7-bis(2,20-bipyridine-5-yl)triphenylene (BPy-TP2) were prepared using procedures given in the literature[6,7] and were further

purified using sublimation. The poly(3,4-ethylenedioxythiophene)-poly(4-stylenesulfonate) (PEDOT:PSS) (AI4083) was purchased from H. C. Stark. 4,4′-Bis(carbazol-9-yl)biphenyl (CBP) and 1,3,5-tris(N-phenylbenzimidazol-2-yl)benzene (TPBI) were purchased from Jilin Optical and Electronic Materials Co., Ltd. All reactions were carried out under a N_2 atmosphere. ^{1}H nuclear magnetic resonance (NMR) and ^{13}C NMR spectra were recorded in $CDCl_3$ by using an Avance III 500 spectrometer (Bruker Biospin, Germany) operating at 500 MHz for ^{1}H NMR and 125 MHz for ^{13}C NMR. High-resolution mass spectrometry (HRMS) by fast atom bombardment was performed using a JEOL JMS-700 spectrometer. Elemental analysis was performed with a Yanaco MT-5 elemental analyser. UV-vis absorption spectra were recorded using a Perkin-Elmer Lambda 950-PKA UV/vis spectrophotometer and photoluminescence spectra were recorded using a Jasco FP-6500 spectrofluorometer equipped with liquid nitrogen attachment. Photoluminescence quantum yields were measured using an absolute photoluminescence (PL) quantum yield measurement system (C11347-01, Hamamatsu Photonics Co., Japan) at an excitation wavelength of 380 nm. The highest occupied molecular orbital (HOMO) energy levels of the compounds in thin film were determined using atmospheric ultraviolet photoelectron spectroscopy using an AC-3 (Riken Keiki). Differential scanning calorimetry (DSC) measurements were carried out on an SII DSC6220 calorimeter under a N_2 atmosphere. The sublimation temperature and thermal decomposition temperature were detected using a thermogravimetry-differential thermal analysis (TG-DTA 2400SA, Bruker, Germany) at a scanning rate of 10 °C/min under vacuum (1 Pa) and in a N_2 atmosphere (1 atm), respectively. Atomic force microscope (AFM) images of the film surfaces were obtained using a JEOL JSPM-5400 scanning probe microscope in tapping-mode in air. The relative density of a vacuum-deposited film was determined from its thickness and relative weight, which were measured by a Dektak 6M surface profilometer (Veeco, Inc.) and a quartz crystal oscillator in the deposition chamber, respectively. All of the calculations were performed using the Gaussian 09 package. The geometries in the ground state were optimized at the DFT(B3LYP)/6-31G* level. The calculations for the vertical transition energies were based on TD-DFT(B3LYP)/6-31G*.

2.2 Synthesis

3-[3-(9-Carbazolyl)phenyl]carbazole (iii): 3-(9-Carbazolyl)phenylboronic acid (**i**) (2.00 g, 7.0 mmol), 3-bromocarbazole (**ii**) (1.43 g, 5.8 mmol), $Pd(PPh_3)_4$ (0.34 g, 0.3 mmol) were mixed in 1,2-dimethoxyethane and stirred under a nitrogen atmosphere. After about 10 min, an aqueous solution of 2 M K_2CO_3 (2.07 g, 15 mmol) was added. After the mixture had been refluxed under nitrogen for 6 hours, it was acidified with dilute HCl and the product was extracted using dichloromethane and water. The organic layer was washed with saturated NaCl and dried over $MgSO_4$. The solvent was then evaporated under vacuum. After recrystallization of the crude product from chloroform, the white product **iii** was obtained (2.32 g, 98%). ^{1}H NMR ($CDCl_3$, 500 MHz): δ [ppm] 8.34 (1H, d, J = 2.0 Hz), 8.18 (2H, d, J = 8.5 Hz), 8.13 (1H, s), 8.11 (1H, d, J = 8.0 Hz), 7.92 (1H, t, J = 2.0 Hz), 7.82 (1H, dt, J = 8.5 Hz, J = 1.0 Hz), 7.73 (1H, dd, J = 8.5 Hz, J = 2.0 Hz), 7.69 (1H, d, J = 8.0 Hz), 7.54–7.50 (4H, m), 7.46–7.42 (4H, m), 7.31 (2H, t, J = 8.0 Hz), 7.27–7.24 (1H, m). ^{13}C NMR ($CDCl_3$, 500 MHz): δ [ppm] 144.0, 141.0, 140.0, 139.2, 138.2, 131.8, 130.2, 126.3, 126.2, 126.0, 125.8, 125.3, 125.0, 124.0, 123.4, 123.4, 120.4, 120.3, 119.9, 119.7, 118.9, 111.0, 110.8, 109.9. HRMS *m/z*: 408 $[M]^+$. Found: C, 88.07; H, 5.06; N, 6.73. Calc. for $C_{30}H_{20}N_2$: C, 88.21; H, 4.93; N, 6.86.

1,3-Bis{3-[3-(9-carbazolyl)phenyl]-9-carbazolyl}benzene (CPCB): 1,3-Diiodobenzene (2.69 g, 8.2 mmol), **iii** (7.04 g, 17.2 mmol), K_2CO_3 (6.8 g, 49 mmol) and copper powder (3.15 g, 49 mmol) were mixed in dimethylformamide and stirred under a nitrogen atmosphere. After the mixture had been refluxed for 72 hours, the product was extracted using dichloromethane and water. The organic layer was washed using saturated NaCl and dried over $MgSO_4$, and then concentrated under vacuum. The residue was purified using column chromatography (hexane/chloroform = 1:3) to obtain a white solid (5.10 g, 70%). The product was further purified by sublimation before use. ^{1}H NMR ($CDCl_3$, 500 MHz): δ [ppm] 8.41 (2H, d, J = 1.5 Hz), 8.18 (2H, d, J = 7.5 Hz), 8.17 (4H, d, J = 7.5 Hz), 7.93 (2H, t, J = 2.0 Hz), 7.90 (1H, t, J = 8.0 Hz), 7.87 (1H, t, J = 2.0 Hz), 7.83 (2H, dt, J = 8.5 Hz, J = 1.5 Hz), 7.75 (4H, dd, J = 8.5 Hz, J = 2.0 Hz), 7.71 (2H, t, J = 8.0 Hz), 7.63 (2H, d, J = 8.5 Hz), 7.57–7.53 (8H, m), 7.47 (2H, td, J = 7.5 Hz, J = 1.2 Hz), 7.43 (4H, td, J = 7.5 Hz, J = 1.2 Hz), 7.33 (2H, t, J = 7.5 Hz), 7.31 (4H, t, J = 7.5 Hz). ^{13}C NMR ($CDCl_3$, 500 MHz): δ [ppm] 143.7, 141.1, 140.9, 140.3, 139.3, 138.2, 132.8, 131.4, 130.3, 129.0, 128.2, 126.5, 126.3, 126.0, 125.9, 125.8, 125.6, 125.2, 124.3, 123.6, 123.4, 120.7, 120.6, 120.3, 119.9, 119.0, 110.1, 109.9. HRMS *m/z*: 890 $[M]^+$. Found: C, 89.04; H, 4.96; N, 5.98 Calc for $C_{66}H_{42}N_4$: C, 88.96; H, 4.75; N, 6.29.

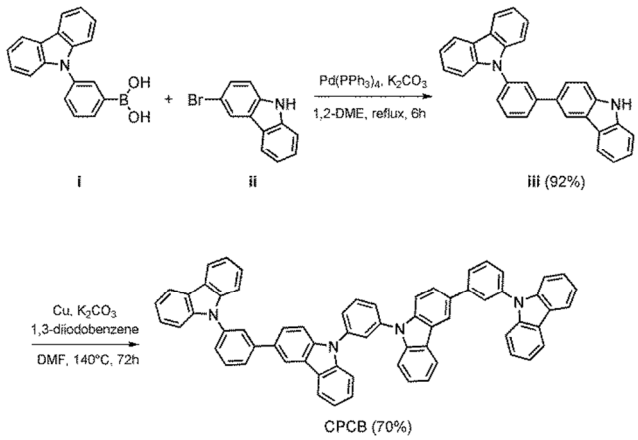

Scheme 1 Synthetic route for CPCB.

2.3 Device fabrication and measurements

A 40-nm-thick PEDOT:PSS layer was spin-coated at 3000 rpm onto a pre-cleaned indium tin oxide (ITO) glass substrate, followed by drying at 200 °C for 10 min. To fabricate the OLEDs with a solution-processed emitting layer, a 30-nm-thick film of 4CzIPN and the host materials were spin-coated at 1500 rpm onto the PEDOT layer from a filtered 5.5 mg/ml dichloromethane or 10.7 mg/mL toluene solution. The films were then annealed under N_2 for 10 minutes. Finally, one or two electron transport layers (ETLs), a LiF layer (0.8 nm) and an Al layer (100 nm) were deposited consecutively onto the spin-coated film in an inert chamber using thermal evaporation at a pressure of $< 4\times10^{-4}$ Pa. The deposition rate of the Al layer was fixed at 0.1 nm s^{-1}, while the deposition rate of the LiF layer was fixed at 0.01 nm s^{-1}. The overlap of the ITO and metal electrodes gave an active device area of 4 mm^2. The fabrication of OLEDs with a dry-processed emitting layer was

the same except that the 4CzIPN and the host materials were co-deposited by thermal vacuum evaporation on the PEDOT:PSS layer. The deposition rate of the organic layers was 0.1 nm s^{-1}. After fabrication, the devices were immediately encapsulated with glass lids using epoxy glue in nitrogen-filled glove boxes (with an O_2 level of 0.1 ppm and a H_2O level of 0.1 ppm). The current density (*J*), voltage (*V*) and luminance (*L*) characteristics of the OLEDs were measured using a Keithley 2400 source meter and an absolute EQE measurement system (C9920-12, Hamamatsu Photonics).

3. Results and discussion

CBP is the most commonly used host material for green PHOLEDs because of its high triplet energy level (2.58 eV) and good bipolar charge mobility.[8,9] However, CBP has a high molecular symmetry and low molecular weight that easily induces crystallization during device operation, leading to rather short lifetimes. Thus, in our previous report, a less symmetrical dimeric 9-phenylcarbazole compound, 3,3-di(9H-carbazol-9-yl)biphenyl (mCBP), was used instead of CBP as a host for the 4CzIPN-based OLED.[2] In combination with an efficient electron transport layer (ETL), fairly good operational stability was demonstrated in vacuum deposited TADF-based OLEDs. Herein a new tetramer of 9-phenylcarbazole, CPCB, was synthesized and employed as a host material for 4CzIPN in solution-processed OLEDs. To limit the conjugation length and maintain a high T_1, the four carbazole units in CPCB were linked to three phenyl bridges via the meta-position.[10] Time-dependent density functional theory (TD-DFT) calculations predicted a T_1 energy level of 3.06 eV at the B3LYP/6-31G* level (Fig. S1), which is higher than that of 2.96 eV for the CBP calculated with the same method.

As shown in Scheme 1, CPCB can be easily synthesized using a two-step coupling reaction, involving a Pd-catalysed Suzuki coupling of 3-(9-carbazolyl)phenylboronic acid (i) and 3-bromocarbazole (ii) followed an Ullmann coupling of the resulting 3-[3-(9-carbazolyl)phenyl]carbazole (iii, 2 equiv.) with 1,3-diiodobenzene (1 equiv.). Detailed methodology for the chemical synthesis and the analytical data are presented in the experimental section.

The absorption and emission spectra of CPCB in toluene at 300 K and 77 K are shown in Fig. 1. The fluorescent band with a maximum of 390 nm at 300 K overlaps with the absorption spectrum of 4CzIPN, implying the presence of efficient Förster

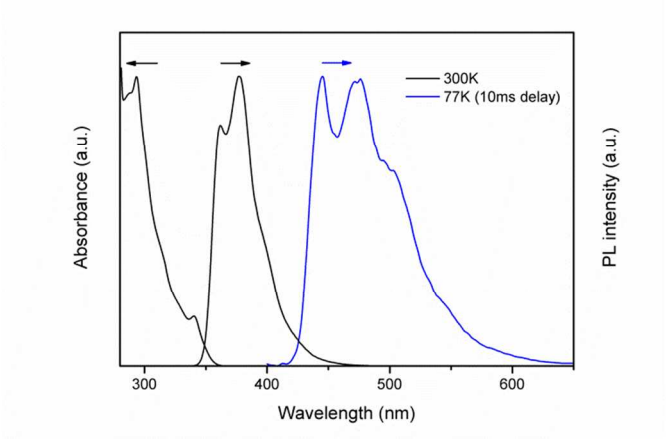

Fig. 1 Absorption and photoluminescence spectra of CPCB in toluene at 300 K and the phosphorescence spectrum in toluene at 77 K using a 10 ms delay.

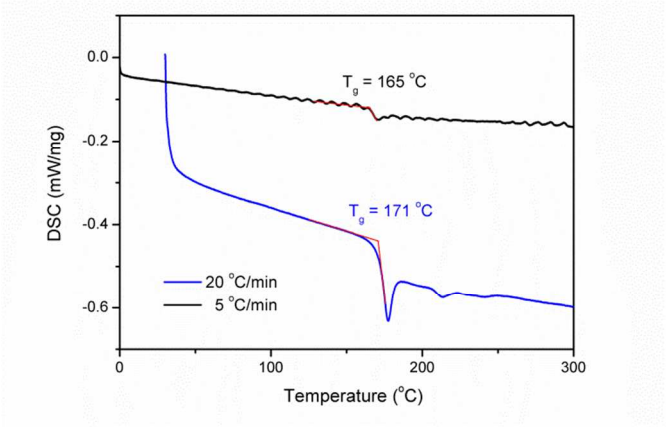

Fig. 2 DSC scans of CPCB recorded at heating rates of 5 °C/min and 20 °C/min. The slower heating rate provided a more accurate glass transition temperature (T_g).

resonance energy transfer from CPCB to 4CzIPN. The T_1 energy level of CPCB (2.79 eV) determined from the highest energy peak of its phosphorescence spectrum (measured at 77 K with a 10 ms delay) is higher than that of the CBP film (2.58 eV),[8] which is consistent with the theoretical prediction. The HOMO level of CPCB was determined to be 6.2 eV using a photo-electron spectroscopy (AC-3) (Fig. S2). The lowest unoccupied molecular orbital (LUMO) level of CPCB was calculated to be 2.7 eV by subtracting the HOMO level from the energy gap determined from the absorption edge (355 nm). Both the HOMO and LUMO levels of CPCB are close those of the CBP film, 6.2 and 2.9 eV, respectively. Although CPCB has

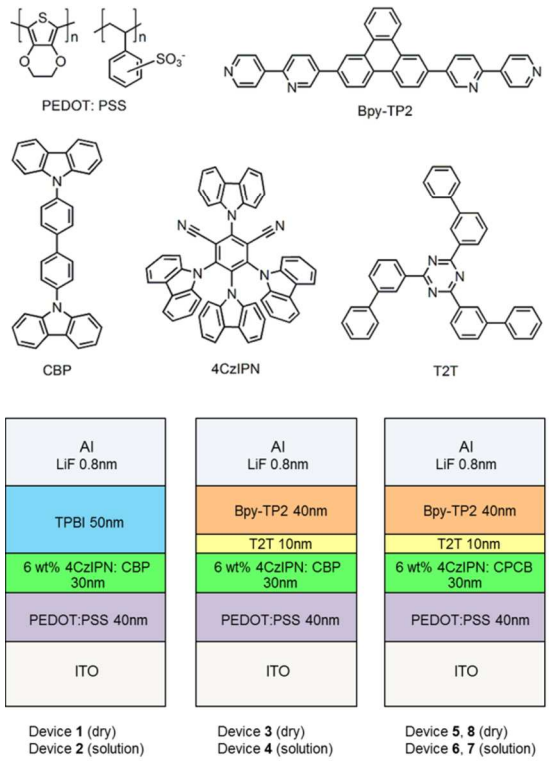

Fig. 3 OLED structures and the compounds. The annealing conditions of the emitting layers are listed in Table 1.

a high sublimation temperature of 394 °C (1 Pa) shown by TG-DTA analysis (Fig. S3), the temperature is still considerably lower than its thermal decomposition temperature, which was found to be higher than 500 °C (Fig. S3). Also, the DSC measurement (Fig. 2) showed that CPCB has a T_g of 165 °C which is much higher than that of 62 °C for CBP,[11] implying high morphological stability of the amorphous film.

CPCB showed good solubility (>5.0 wt%) in many polar solvents such as toluene, tetrahydrofuran and dichloromethane. A high PLQY of 86% was observed in the spin-coated film of 6 wt% 4CzIPN:CPCB, which is as high as that of 6 wt% 4CzIPN:CBP film fabricated by either vacuum deposition or spin-coating. These characteristics indicate that CPCB should provide a good host for 4CzIPN in solution-processed OLEDs. Herein, we compared the EL properties of 4CzIPN-based OLEDs with a CBP or a CPCB host. The three main device structures are shown in Fig. 3. For each device structure, the EML was fabricated by both dry (**1**, **3**, **5**, **8**) and solution (**2**, **4**, **6**, **7**) processes. For the solution-processed OLEDs, an annealing step was used to remove residual solvent in the EMLs after spin-coating.[12]

Device **1** had a spin-coated 40-nm-thick hole injection layer (HIL) of PEDOT:PSS and vacuum-deposited 30-nm-thick EML of 6 wt% 4CzIPN:CBP and a 50-nm-thick ETL of TPBI. The main difference between this device and the device previously reported[1f] is the different HILs. Interestingly, it was found that replacement of the vacuum-deposited 4,4-bis[N-(1-naphthyl)-N-phenylamino]biphenyl (α-NPD) layer with a PEDOT:PSS layer had little effect on the device performance. As shown in Fig. 4, the EL of device **1** turned on at 3.4 V with an emission maximum at 510 nm. The EQE at 1.0, 10, 100 mA/cm^2 was 18.0%, 12.3% and 4.8% respectively. All these values are almost the same as the reference device with an α-NPD HIL layer.[1f] Device **2** was prepared by employing the same device structure but preparing the EML by spin-coating a mixture of 4CzIPN and CBP in dichloromethane onto a PEDOT:PSS layer. Device **2** had a similar performance. The EL spectrum, current density-voltage and EQE-current density characteristics of device **2** are almost the same as those of device **1**. However, both dry- and solution-processed OLEDs with this structure had a very short operational lifetime. The half-life (LT50) of devices **1** and **2** were 6.2 and 2.2 hours, respectively, with an initial luminescence at about 1000 cd/m^2 (EQE≈17%). The poor device stability may be because of the narrow carrier recombination zone located at the interface between the EML and ETL (TPBI).[2]

To improve the operational lifetime, we replaced the TPBI layer with a 10-nm-thick T2T and a 40-nm-thick BPy-TP2 layer in device **1** and **2** (Fig. 3), and fabricated two T2T/BPy-TP2-based OLEDs using dry-processed and solution-processed EMLs (6 wt% 4CzIPN:CBP). Herein, T2T is used as an exciton blocking layer because of its high T_1 energy level and good electron mobility,[6] and BPy-TP2 is used as an ETL because of its high electron mobility resulting from a highly ordered

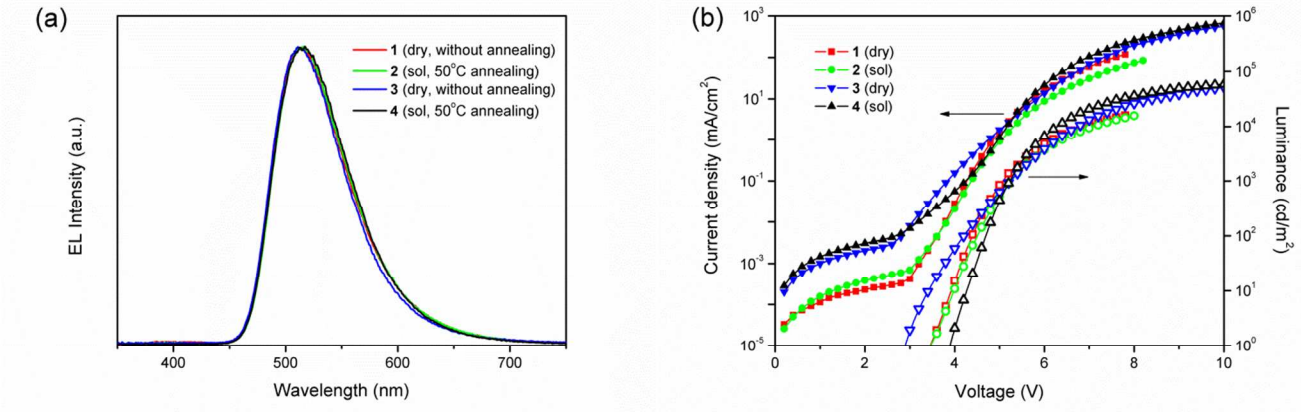

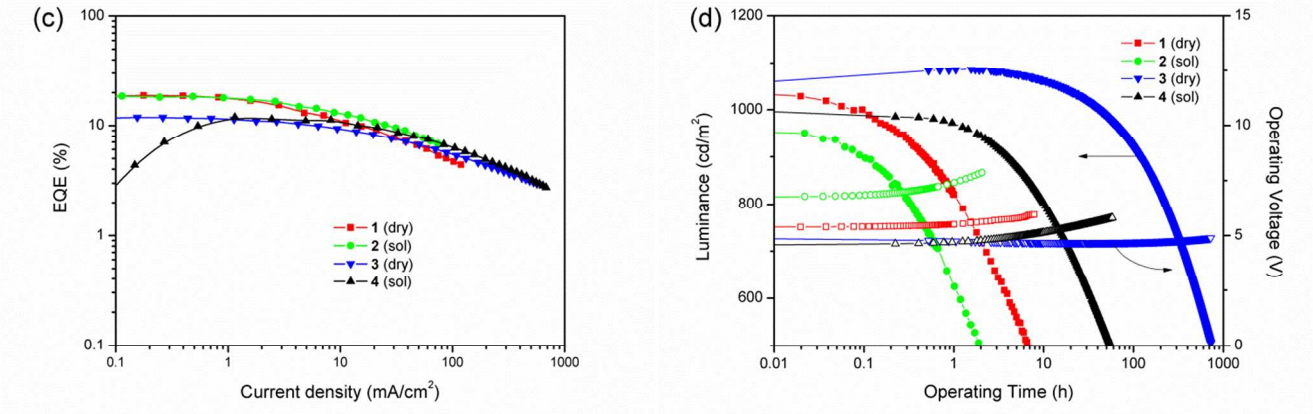

Fig. 4. **(a)** EL spectra at 10 mA/cm^2; **(b)** luminance-current density-voltage characteristics; **(c)** EQE-current density characteristics; and **(d)** luminance-voltage-operating time characteristics at fixed current densities for devices **1**–**4**. The preparation methods of the emissive layers are given in Table 1. The annealing time was fixed at 10 min.

Table 1. Device structure, preparation method of the emissive layer (EML), the maximum external quantum efficiency (EQE_{max}), the external quantum efficiency (EQE_{1000}) and voltage (V_{1000}) at a luminescence of 1000 cd/m^2, and the half-life (LT50) of TADF-based OLEDs using 4CzIPN as the emissive layer.

Device	EML (preparation)/ETL	Anneal of EML[a]	EQE_{max} (%)	EQE_{1000} (%)	V_{1000} (V)	LT50 [b] (h)
1	CBP: 4CzIPN (dry)/TPBI	no	18.8	16.8	5.1	6.2
2	CBP: 4CzIPN (sol)/TPBI	50ºC [c]	18.5	17.2	5.3	2.2
3	CBP: 4CzIPN (dry)/T2T/BPyTP2	no	11.8	10.9	5.2	680
4	CBP: 4CzIPN (sol)/T2T/BPyTP2	50ºC	11.9	11.4	5.2	56
5	CPCB: 4CzIPN (dry)/T2T/BPyTP2	no	14.5	12.7	6.0	208
6	CPCB: 4CzIPN (sol)/T2T/BPyTP2	220ºC	9.9	9.8	5.3	184
7	CPCB: 4CzIPN (sol)/T2T/BPyTP2	180ºC	9.1	9.1	5.3	82
8	CPCB: 4CzIPN (dry)/T2T/BPyTP2	220ºC	11.6	11.6	5.2	600

[a] The time of each annealing process is fixed at10 min; [b] The initial luminances are about 1,000 cd/m^2; [c] The effect of annealing temperature on the device properties is shown in Fig. S4.

molecular orientation.[7] As expected, the T2T/BPy-TP2-based OLEDs had a higher current density and much longer LT50 (680 h for **3** and 56 h for **4**) compared with the TPBI-based OLEDs. However, the maximum EQE of devices **3** and **4** (~12%) is considerably lower than that of devices **1** and **2** (Fig. 4). These deteriorations can be attributed to the improved electron transport in the ETL and injection into the EML from the T2T/BPy-TP2 layer. This resulted in an increase of the electron current and enlargement of the carrier recombination zone from the EML/ETL interface to the bulk of the EML, providing significant improvement of the device lifetime. However, the approach of the carrier recombination zone towards the PEDOT:PSS layer will result in the loss of excitons because the lower S_1 (~1.6 eV)[13] and T_1 energy levels of the PEDOT:PSS will quench singlet and triplet excitons by Förster and Dexter processes, respectively. In this case, inserting an exciton blocking layer between the HIL and the EML would enhance device efficiency.

Although the operational lifetime of the solution-processed OLED based on the T2T/BPy-TP2 layers (**4**) is 25 times as long as the OLED based on the TPBI layer (**2**), it is still much shorter than that of the dry-processed OLED with the same structure (**3**). To investigate the surface morphologies, we fabricated spin-coated and vacuum-deposited EML films of 6 wt% 4CzIPN:CBP layer onto a PEDOT:PSS layer. AFM images of these two films are shown in Fig. 5. The root-mean-square (RMS) surface roughness values of the spin-coated and the

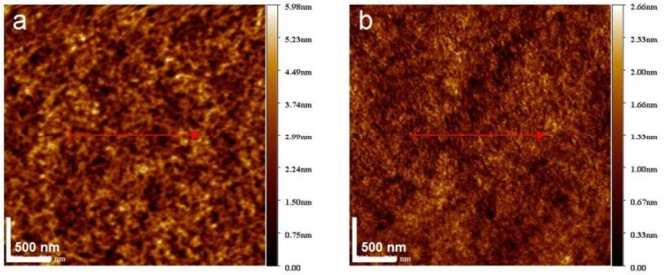

Fig. 5 AFM images of **(a)** 30-nm-thick vacuum deposited and **(b)** spin-coated films of a 6 wt% 4CzIPN: CBP layer on a PEDOT:PSS coated ITO substrates. The spin-coated film was prepared using CH_2Cl_2 as the solvent and was then annealed at 50 °C for 10 min. The RMS roughness of the dry-processed film was 0.70 nm and was 0.27 nm for the solution-processed film.

vacuum-deposited EML film were 0.27 and 0.70 nm, respectively, indicating that the spin-coated film has smoother surface than the vacuum-deposited film, which is consistent with the previous study reported by Shinar *et al.*[5i] We assumed that lower reliability of the solution-processed OLED compared with the dry-processed OLED would be attributed to the ease of crystallization of the CBP in the solution-processed film during device operation, just as that in ambient conditions (Fig. S5).

One can assume that the small and symmetrical CBP molecule easily forms nanometre-sized ordered clusters during the spin-coating process, which would induce the crystallization of CBP with elevated device temperature under operational conditions.[14] Another possibility is that the density of the solution-processed films is smaller than the dry-processed film after removing the solvent by annealing,[5e] and therefore the CBP molecules can move more easily and crystallize in the solution-processed film. Accordingly, high triplet energy host materials with a larger molecular weight and greater solubility should be used in solution-processed OLEDs.

In comparison with CBP, CPCB has a higher molecular weight and broader conformational distribution, leading to a better solubility in many common solvents. By depositing a 6 wt% 4CzIPN:CPCB film on a PEDOT:PSS coated ITO substrate by dry (**5**) or solution (**6**) processing, two CPCB-based OLEDs were fabricated with a similar structure to the CBP-based devices (structures **3** and **4**). For device **6**, the EML was annealed at 220 °C for 10 min after spin-coating. As shown in Fig. 6, the EQEs for device **5** and **6** at 1000 cd/m^2 were 12.7% and 9.8%, respectively, which are comparable to that of the CBP-based counterparts (~11%). As expected, the solution-processed device using a CPCB host layer (**6**) is more reliable than the similar device using CBP host (**4**). The LT50 of device **6** at an initial luminance of ~1000 cd/m^2 is 184 hours, corresponding to that of 56 hours for device **4**. Although the EQE and LT50 of this optimized solution-processed 4CzIPN-based OLED (**6**) at an initial luminance of 1000 cd/m^2 are still lower than those of the optimized dry-processed 4CzIPN-based OLEDs[2] they are significantly improved with respect to previously reported solution-processed green PHOLEDs.[5c,5e]

It was unexpected to find that the dry-processed CPCB-based OLED (**5**) has a shorter LT50 of 208 hours relative to that of 680 hours for the dry-processed CBP-based OLED (**3**). Also, the current density of device **5** was significantly lower than devices **3** and **6**. The lower current density and LT50 of device **5** relative to device **3** may be attributed to the loosely packed EML mainly consisting of bar-shaped CPCB molecules. The

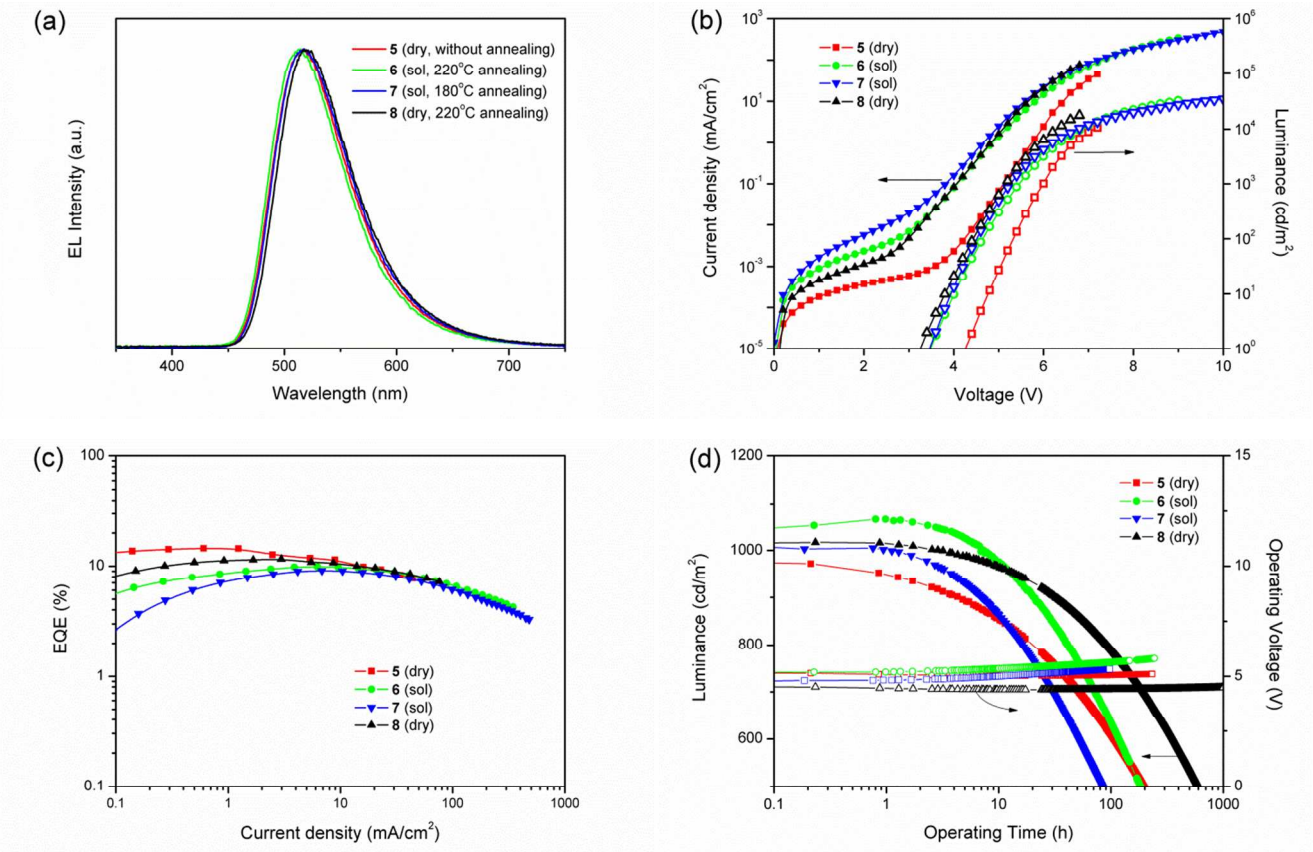

Fig. 6 **(a)** EL spectra at 10 mA/cm^2; **(b)** luminance-current density-voltage characteristics; **(c)** EQE-current density characteristics; and **(d)** luminance-voltage-operating time characteristics at fixed current densities for devices **5–8**. The preparation methods of the emissive layers are given in Table 1. The annealing time was fixed at 10 min.

relative density of a vacuum-deposited CPCB layer was found to be 90% of that of a vacuum-deposited CBP layer. Since an annealing process can enhance the current density as well as the stability of a device by improving the intermolecular interaction in organic layers and the interfacial adhesion between adjacent layers (Fig. S4), a control device (**8**) with the same structure as device **5** was fabricated by annealing the vacuum-deposited 4CzIPN:CPCB layer at 220 °C for 10 min before the deposition of following layers. Device **8** showed an increase in the current density as well as a prolonged LT50 of 600 hours (Fig. 6), which is comparable with that of the dry-processed CBP-based OLED (**3**).

Conclusions

In short, we demonstrated that solution-processed TADF-based OLEDs with a 4CzIPN emitter and a CBP host achieved EQEs as high as the dry-processed OLEDs with the same structures. However, the operational lifetime of the solution-processed device was much shorter than that of the dry-processed device because of a poor morphological stability of the spin-coated CBP film. Increasing the molecular weight of the carbazole-based host material without lowering its T_1 level could significantly improve the operational stability. Also, avoiding the recombination of holes and electrons near the interface between the hole-transport and the ETL is key to realizing long-lifetime reliability. Since we did not use an exciton blocking layer between the emissive layer and the PEDOT:PSS layer, the TADF-based OLEDs had a limited EQE of ~12% in this study. Developing cross-linkable hole-transport materials with a high T_1 energy will enhance OLED performance.

Acknowledgements

This work was supported in part by the Funding Program for World-Leading Innovative R&D on Science and Technology (FIRST) and the Exploratory Research for Advanced Technology (ERATO). The authors would like to acknowledge Dr. Kazunori Togashi, Ms. Nozomi Nakamura, Ms Keiko Kusuhara and Ms. Hiroko Nomura for the synthesis and purification of Bpy-TP2, 4CzIPN and T2T. The authors also acknowledge Mr. Masaki Numata, Mr. Takehiro Takahashi, Dr. Junichi Nishide and Mr. Hiroshi Miyazaki for their support in this study.

Notes and references

[a] *Center for Organic Photonics and Electronics Research (OPERA) and Center for Future Chemistry, Kyushu University, 744 Motooka, Nishi, Fukuoka 819-0395, Japan. Email: adachi@cstf.kyushu-u.ac.jp; Fax: +81-92-802-6921; Tel: +81-92-802-6920*

[b] *Sumitomo Riko Company, Ltd., Material Technology R&D Laboratories, 1 Higashi 3-chome, Komaki, Aichi 485-8550, Japan*

Electronic Supplementary Information (ESI) available: [molecular orbital and TG-DTA data; photoelectron yield and NMR spectra]. See DOI: 10.1039/b000000x/

1 (a) A. Endo, K. Sato, K. Yoshimura, T. Kai, A. Kawada, H. Miyazaki and C. Adachi, *Appl. Phys. Lett.*, 2011, **98**, 083302; (b) K. Goushi, K. Yoshida, K. Sato and C. Adachi, *Nat. Photonics*, 2012, **6**, 253; (c) T. Nakagawa, S.-Y. Ku, K.-T. Wong and C. Adachi, *Chem. Commun.*, 2012, **48**, 9580; (d) Q. Zhang, J. Li, K. Shizu, S. Huang, S. Hirata, H. Miyazaki and C. Adachi, *J. Am. Chem. Soc.*, 2012, **134**, 14706; (e) H. Tanaka, K. Shizu, H. Miyazakiab and C. Adachi, *Chem. Commun.*, 2012, **48**, 11392; (f) H. Uoyama, K. Goushi, K. Shizu, H. Nomura and C. Adachi, *Nature*, 2012, **492**, 234; (g) J. Li, T. Nakagawa, J. MacDonald, Q. Zhang, H. Nomura, H. Miyazaki and C. Adachi, *Adv. Mater.*, 2013, **25**, 3319; (h) F. B. Dias, K. N. Bourdakos, V. Jankus, K. C. Moss, K. T. Kamtekar, V. Bhalla, J. Santos, M. R. Bryce and A. P. Monkman, *Adv. Mater.*, 2013, **25**, 3707; (i) Q. Zhang, B. Li, S. Huang, H. Nomura, H. Tanaka, C. Adachi, *Nat. Photonics*, 2014, **8**, 326; (j) J. W. Sun, J.-H. Lee, C.-K. Moon, K.-H. Kim, H. Shin and J.-J. Kim, *Adv. Mater.*, 2014, **26**, 5684; (k) H. Wang, L. Xie, Q. Peng, L. Meng, Y. Wang, Y. Yi and P. Wang, *Adv. Mater.*, 2014, **26**, 5198.

2 H. Nakanotani, K. Masui, J. Nishide, T. Shibata and C. Adachi, *Sci. Rep.*, 2013, **3**, 2127.

3 (a) J. H. Burroughes, D. D. C. Bradley, A. R. Brown, R. N. Marks, K. Mackay, R. H. Friend, P. L. Burns, A. B. Holmes, *Nature*, 1990, **347**, 539; (b) G. Gustafsson, Y. Cao, G. M. Treacy, F. Klavetter, N. Colaneri, A.J. Heeger, *Nature*, 1992, **357**, 477; (c) F. So, B. Krummacher, M. K. Mathai, D. Poplavskyy, S. A. Choulis, V.-E. Choong, *J. Appl. Phys.*, 2007, **102**, 091101.

4 (a) W.-Y. Wong and C.-L. Ho, Coord. Chem. Rev., 2009, **253**, 1709; (b) X. Gong, M. R. Robinson, J. C. Ostrowski, D. Moses, G. C. Bazan and A. J. Heeger, *Adv. Mater.*, 2002, **14**, 581; (c) S.-C. Lo, N. A. H. Male, J. P. J. Markham, S. W. Magennis, P. L. Burn, O. Salata and I. D. W. Samuel, *Adv. Mater.*, 2002, **14**, 975; (d) H. Wu, G. Zhou, J. Zou, C.-L. Ho, W.-Y. Wong, W. Yang, J. Peng and Y. Cao, *Adv. Mater.*, 2009, **21**, 4181; (e) S. Shao, J. Ding, L. Wang, X. Jing and F. Wang, *J. Am. Chem. Soc.*, 2012, **134**, 20290; (f) D. Xia, B. Wang, B. Chen, S. Wang, B. Zhang, J. Ding, L. Wang, X. Jing and F. Wang, *Angew. Chem. Int. Ed.*, 2014, **53**, 1048.

5 (a) L. Duan, L. Hou, T.-W. Lee, J. Qiao, D. Zhang, G. Dong, L. Wang and Y. Qiu, *J. Mater. Chem. C.*, 2010, **20**, 6392; (b) K. S. Yook and J. Y. Lee, *Adv. Mater.*, 2014, **26**, 4218; (c) M. Ooe, S. Naka, H. Okada and H. Onnagawa, *Jpn. J. Appl. Phys.*, 2006, **45**, 250; (d) Q. Zhang, Y. Cheng, L. Wang, Z. Xie, X. Jing and F. Wang, *Adv. Funct. Mater.* 2007, **17**, 2983; (e) T.-W. Lee, T. Noh, H.-W. Shin, O. Kwon, J.-J. Park, B.-K. Choi, M.-S. Kim, D. W. Shin and Y.-R. Kim, *Adv. Func. Mater.*, 2009, **19**, 1625; (f) J.-H. Jou, W.-B. Wang, S.-Z. Chen, J.-J. Shyue, M.-F. Hsu, C.-W. Lin,S.-M. Shen, C.-J. Wang, C.-P. Liu, C.-T. Chen, M.-F. Wud and S.-W. Liu, *J. Mater. Chem.*, 2010, **20**, 8411; (g) W. Jiang, L. Duan, J. Qiao, D. Zhang, G. Dong, L. Wang and Y. Qiu, *J. Mater. Chem.*, 2010, **20**, 6131; (h) K. S. Yook and J. Y. Lee, *Org. Electron.*, 2011, **12**, 1711; (i) M. Cai, T. Xiao, E. Hellerich, Y. Chen, R. Shinar and J. Shinar, *Adv. Mater.*, 2011, **23**, 3590. (j) H.-C. Yeh, H.-F. Meng, H.-W. Lin, T.-C. Chao, M.-R. Tseng, H.-W. Zan, *Org. Electron.*, 2012, **13**, 914.

6 H.-F. Chen, S.-J. Yang, Z.-H. Tsai, W.-Y. Hung, T.-C. Wang and K.-T. Wong, *J. Mater. Chem.*, 2009, **19**, 8112.

7 K. Togashi, S. Nomura, N. Yokoyama, T. Yasudaabc and C. Adachi, *J. Mater. Chem.*, 2012, **22**, 20689.

8 (a) C. Adachi, R. C. Kwong, P. Djurovich, V. Adamovich, M. A. Baldo, M. E. Thompson and S. R. Forrest, *Appl. Phys. Lett.*, 2001, **79**, 2082; (b) S. Reineke and M. A. Baldo, *Sci. Rep.*, 2014, **4**, 3797.

9 (a) H. Kanai, S. Ichinosawa and Y. Sato, *Synth. Met.*, 1997, **91**, 195; (b) T. Yamada, F. Suzuki, A. Goto, T. Sato, K. Tanaka and H. Kaji, *Org. Electron.*, 2011, **12**, 169.

10 A. Köhler and H. Bässler, *Mater. Sci. Eng. R*, 2009, **66**, 71.

11 M.-H. Tsai, Y.-H. Hong, C.-H. Chang, H.-C. Su, C.-C. Wu, A. Matoliukstyte, J. Simokaitiene, S. Grigalevicius, J. V. Grazulevicius and C.-P. Hsu, *Adv. Mater.*, 2007, **19**, 862.

12 G. Mao, Z. Wu, Q. He, B. Jiao, G. Hu, X. Hou, Z. Chen and Q. Gong, *Appl. Surf. Sci.*, 2011, **257**, 7394.

13 Q. Pei, G. Zuccarello, M. Ahskog and O. Inganäs, *Polymer*, 1994, **35**, 1347.

14 (1) X. Zhou, J. He, L. S. Liao, M. Lu, X. M. Ding, X. Y. Hou, X. M. Zhang, X. Q. He and S. T. Lee, *Adv. Mater.*, 2000, **12**, 265; (2) F. So and D. Kondakov, *Adv. Mater.*, 2010, **22**, 3762.

Table of contents entry

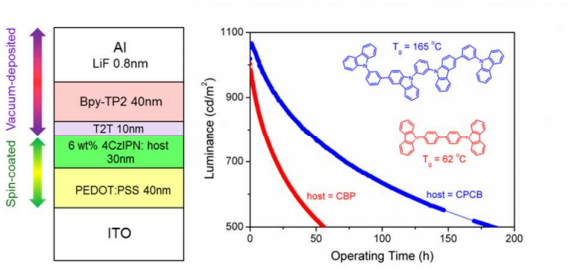

Stability of solution-processed organic light-emitting diodes employing a thermally activated delayed fluorescent emitter was improved using a host with a high glass transition temperature and high mobility electron transport layers.